Inorg. Chem. **2003**, *42*, 5015–5022

Investigation of the Interaction between 1-Hydroxyethane-1,1′-diphosphonic Acid (HEDP) and Uranium(VI)

Christophe Jacopin,*,† Marcin Sawicki,‡ Gabriel Plancque,† Denis Doizi,† Frédéric Taran,‡ Eric Ansoborlo,§ Badia Amekraz,† and Christophe Moulin*,†

CEA-Saclay, DEN/DPC/SECR/LSRM, 91191 Gif-sur-Yvette Cedex, France, CEA-Saclay, DSV/DBJC/SMMCB, 91191 Gif-sur-Yvette Cedex, France, and CEA-Valrhô, DEN/VRH/DRCP/CETAMA/DIR, 30207 Bagnols-sur-Cèze Cedex, France

Received April 1, 2003

A detailed study, using a panel of spectroscopic analytical methods, of the complexation between 1-hydroxyethane-1,1′-diphosphonic acid (HEDP) and uranyl ion (UO_2^{2+}) is reported. Results suggest that the metal complex is present as only 1:1 (metal/ligand) species at low concentration ($<10^{-4}$ M). The conditional constants of this complex were determined at various pH using time-resolved laser-induced fluorescence (TRLIF) and electrospray ionization mass spectrometry (ESI-MS). Further investigations indicate the presence of a 1:2 (metal/ligand) complex at higher concentrations ($\sim 10^{-2}$ M). Selectivity studies as well as structural aspects are presented.

Introduction

During the last years, a great deal of work has been devoted to the development of new compounds or ligands to increase the natural rate of elimination of uranium from the human body and to reduce the fixation within target organs (kidney, bone).[1−8] The principle of chelating agent efficiency is that the agent combines with the metal to form a stable complex that can be easily excreted and thus reduces the radiation doses delivered to sensitive cells or organs and the risk of delayed radiation effects, such as cancer. Soluble uranyl ion (UO_2^{2+}) or uranium(VI) is known to be a kidney poison.[9] It also accumulates in bone where a high dose of radiation of some uranium isotopes (^{234}U, ^{233}U) can induce bone cancer. Although numerous studies have been carried out since the 1940s, ligands that efficiently and stably bind UO_2^{2+} at pH corresponding to biological barriers, promote its excretion, and reduce significantly deposits in kidneys and bones remain to be discovered.[10] Some promising ligands were synthesized and tested such as 5-LI(Me-3,2-HOPO) (hydroxypyridinoate function), which shows significant decrease in the kidney, or 5-LICAM(S) (catecholate function), which induces significant decrease in the bone: a combination of two ligands is recommended. Because their toxicity is not well defined,[11] the only used and recommended treatment, up to now, is intravenous administration of bicarbonate.

Bisphosphonates are known to reduce the rate of bone turnover, that is, the rate of removal and replacement of bone tissue. Because phosphonates are hardly biodegradable, chemical speciation based on numerous chemical equilibrium data are of great importance for such applications as environmental fields, waste management, agriculture, scale inhibition, magnetic resonance imaging, behavior of radiopharmaceuticals in blood plasma, or decorporation. Among them, 1-hydroxyethane-1,1′-diphosphonic acid (HEDP) is a therapeutic agent that is widely used in the treatment of

* Authors to whom correspondence should be addressed. Phone: +33-1-69088348. Fax: +33-1-69085411. E-mail: jacopin@carnac.cea.fr (C.J.); moulin@carnac.cea.fr (C.M.).
† CEA-Saclay, DEN.
‡ CEA Saclay, DSV.
§ CEA-Valrhô.

(1) Durbin, P. W.; Kullgren, B.; Xu, J. D.; Raymond, K. N. *Radiat. Prot. Dosim.* **1998**, *79*, 433.
(2) Basinger, M. A.; Forti, R. L.; Burka, L. T. *J. Toxicol. Environ. Health* **1983**, *64*, 237.
(3) Ortega, H.; Domingo, J. L.; Gomez, M.; Corbella *J. Pharmacol. Toxicol.* **1989**, *64*, 247.
(4) Stradling, G. N.; Gray, S. A.; Moody, J. C.; Ellender, M. *Hum. Exp. Toxciol.* **1991**, *10*, 195.
(5) Taylor, D. M.; Sradling, G. N.; Hengé-Napoli, M. H. *Radiat. Prot. Dosim.* **2000**, *87*, 1, 11.
(6) Bailly, T.; Burgada, R.; Stradling, G. N.; Gray, S. A. *EULEP Newsl.* **1994**, *75*, 37.
(7) Hengé-Napoli, M. H.; Ansoborlo, E.; Houpert, P.; Mirto, H.; Paquet, F.; Burgada, R.; Hodgson, S. A.; Stradling, G. N. *Radiat. Prot. Dosim.* **1998**, *79*, 449.
(8) Hengé-Napoli, M. H.; Archimbaud, M.; Ansoborlo, E.; Métivier, H.; Gourmelon, P. *Int. J. Radiat. Biol.* **1995**, *68*, 389.
(9) Leggett, R. W. *Health Phys.* **1989**, *57*, 365.
(10) Stradling, G. N.; Hengé-Napoli, M. H.; Paquet, F.; Poncy, J. L.; Fritsch, P.; Taylor, D. M. *Radiat. Prot. Dosim.* **2000**, *87*, 29.
(11) Durbin, P. W.; Kullgreen, B.; Ebbe, S. N.; Xu, J.; Raymond, K. N. *Health Phys.* **2000**, *78*, 511.

10.1021/ic0343509 CCC: $25.00
Published on Web 07/18/2003

osteopenic diseases.[12] Its toxicology was well studied and revealed an appropriate biocompatibility, and it has a clinical acceptance for this application. Moreover, HEDP has been demonstrated to interact with uranium in vitro and in vivo where it has been shown to be effective as a decontaminating agent after cutaneous contamination[13−14] and in preventing the inhibition of bone formation induced after acute uranium intoxication. HEDP is able to counteract the effect of lethal doses of uranyl nitrate in young rats[15−16] and to complex uranium bound to its biological carriers in the blood and in the kidneys. The in vivo results showed a better efficiency compared with the other ligand such as 3,4,3-LI(1,2-HOPO).[17] The uranyl ion, UO_2^{2+} (U(VI)), is the most stable U species in solution and the most likely form of U to be present in body fluids. In plasma, approximately 40% of U is present as a transferrin complex and 60% as low-molecular-weight anionic complexes. The low-molecular-weight complexes are filtered rapidly at the glomerulus, and the weak U-transferrin complex, which is not filterable, dissociates as the low-molecular-weight U complexes in plasma are depleted. The toxic action of U(VI) on the kidneys is not fully understood, but several potentially important, interrelated events have been identified. For example, U damages the kidneys by binding to the luminal membranes of renal tubular cells, interfering with reabsorption of glucose, sodium, amino acids, protein, water, and other substances, and causing slow cell death by suppression of respiration.[18] These studies have shown that HEDP is able to interact with the uranyl ion at pH 5, corresponding to the pH of the kidney. Although, this efficiency needs to be confirmed, HEDP appears as a promising candidate for human decorporation of uranium. Several stability constants were reported for the complexes of HEDP with Fe(III), Cr(III) and Al(III),[19] Eu-(III), Cu(II),[20] and twelve metal ions, including the alkaline earth and transition and nontransition metal ions.[21] In the last case, the results reveal that only monuclear (1:1) di-, mono-, and unprotonated metal chelates are formed. Regarding UO_2^{2+}, an extensive series of solvent extraction distribution experiments was performed to determine the complex stability and stoichiometries with a panel of phosphonates (MDPA, VDPA, HEDPA, E12DPA, and CMPA).[22] The results show the formation of the 1:1 complexes at low concentration, and at higher pH and concentration, the 1:2 complexes are dominant. The complexation of the uranyl ion with aminomethylenediphosphonates MAMDP and AMDP were also reported.[23] The goal of this study was first to determine the stoichiometry of the uranyl−HEDP complex, as well as to determine the conditional constant at various pH and stability constant using two complementary speciation techniques, that is, time-resolved laser-induced fluorescence and electrospray mass spectrometry (TRLIF, ESI-MS) in homogeneous medium. In a second part, nuclear magnetic resonance (NMR) and attenuated total reflection infrared (ATR-IR) spectroscopy have been used to obtain structural information of the complex. Finally, the selectivity of HEDP toward UO_2^{2+} compared to Na^+, K^+, Ca^{2+}, and Mg^{2+} present at high levels in biological fluids was examined.

Experimental Section

Time-Resolved Laser-Induced Fluorescence (TRLIF). A Nd:YAG laser (model Minilite, Continuum, Santa Clara, CA) operating at 266 nm (quadrupled) or 355 nm (tripled) and delivering an energy of 2 mJ in a 4 ns pulse duration at a repetition rate of 15 Hz was used as the excitation source. The laser output energy is monitored by a laser powermeter (Scientech, Boulder, CO). The excitation laser beam is focused on the cell of the spectrofluorometer "Fluo 2001" (Dilor, France). The light emitted from the cell is focused onto the entrance slit of the polychromator. Taking into account dispersion of the holographic grating used in the polychromator, measurement range extends approximately 200 nm into the visible spectrum with a resolution of 1 nm. The detection is performed by an intensified array of photodiodes (1024 diodes) cooled by Peltier effect (−35 °C) and positioned at the polychromator exit. Recording of spectra was performed by integration of the pulsed light signal given by the intensifier. The integration time is adjustable from 1 to 99 s and allows for variation in detection sensitivity. Logic circuits, synchronized with the laser shot, allow the intensifier to be active with a defined time delay and during a selected aperture time. The whole system is controlled by a microcomputer. Only one gate delay and duration was used to certify the presence of only one complex by the measurement of a single fluorescence lifetime and spectrum. The gate delay used was 250 μs, the gate length was 100 μs, and the integration time was 0.5 s. The emission wavelength was 519 nm (excitation at 266 nm), and the temperature was 20 °C.

MS Apparatus and Conditions. Electrospray ionization mass spectrometric detection of positive and negative ions was performed by using a Quattro (Micromass, Manchester, U.K.) mass spectrometer. The samples were introduced into the source with a syringe pump (Harvard Apparatus, Cambridge, MA). Nitrogen was employed as both the drying and spraying gas with a source temperature of 80 °C. The cone voltage was set to 30 and 60 V, the voltage applied on the capillary is 3500 kV, and the sample solution flow rate was 10 μL min^{-1}. Spectra were recorded by averaging 40 scans from 100 to 1000 *m*/*z* at a scan rate of 6 s/scan. The prepared samples are the same those used in TRLIF. In the positive and negative mode, spectra are acquired at various pH by using different cone voltages which allows to visualization of the complex and the associate cluster.

(12) Harris, S. T. *Osteoporosis Int.* **2001**, *12*, 3, s11−6.
(13) Tymen, H.; Hoffschir, D.; Gerasimo, P.; Marty, J. P. *Ann. Pharm. Fr.* **2000**, *58*, 405.
(14) Tymen, H.; Gerasimo, P.; Hoffschir, D. *Int. J. Radiat. Biol.* **2000**, *76*, 1417.
(15) Ubios, A. M.; Braun, E. M.; Cabrini, R. L. *Health Phys.* **1994**, *66*, 540.
(16) Martinez, A. B.; Cabrini, R. L.; Ubios, A. M. *Health Phys.* **2000**, *78*, 668.
(17) Hengé-Napoli, M. H.; Ansoborlo, E.; Chazel, V.; Houpert, P.; Paquet, F.; Gourmelon, P. *Int. J. Radiat. Biol.* **1999**, *75*, 1473.
(18) (a) Hodge, H. C. In *Pharmacology and toxicology of uranium compounds*; Voegtlin, C.; Hodge, H. C., Eds. National Nuclear Energy Series, Division VI, Vol. I, Part IV; McGraw-Hill: New York, 1953; Chapters 18−28, pp 2335−2423. (b) Passow, H.; Rothstein, A.; Clarkson, T. W. The general pharmacology of the heavy metals. *Pharmacol. Rev.* **1961**, *13*, 186−224. (c) Leggett, R. W. *Health Phys.* **1989**, *57*, 365.
(19) Lacour, S.; Deluchat, V.; Bollinger, J. C.; Serpaud, B. *Talanta* **1998**, *46*, 999.
(20) (a) Nash, K. L.; Rao, L. F.; Chopin, G. R. *Inorg. Chem.* **1995**, *34*, 2753. (b) Vassershtein, Sh. E.; Van Nam, N. *Russ. J. Inorg. Chem.* **1973**, *18*, 4, 541.
(21) Rizkalla, E. N.; Zaki, M. T. M.; Ismail, M. I. *Talenta* **1980**, *27*, 715.
(22) Nash, K. L. *Radiochim. Acta* **1993**, *61*, 147.
(23) Bollinger, J. E.; Roundhill, D. M. *Inorg. Chem.* **1994**, *33*, 6421.

Attenuated Total Reflection Infrared (ATR−IR) Spectroscopy. An unheated "Golden Gate" spectrometer (diamond crystal with an incident angle of 45°, ZnSe focusing lenses) was used at atmospheric pressure. The ATR FT-IR spectra were recorded with the use of a Bruker IFS 55 FT-IR spectrometer with a DTGS detector. The spectra were calculated after 50 scans taken at a resolution of 2 cm^{-1} using Opus OS2 software (Bruker).

NMR. The UO_2^{2+}−HEDP complex was prepared by adding HEDP into a solution of UO_2^{2+} in CD_3OD (20 mM) at different ratios (R) of 1:1; 1:2; 1:5, and 1:10. All measurements were made at room temperature. ^{31}P spectra were obtained using a Brucker MSL 300 spectrometer (121.5 MHz for ^{31}P). The external standard, placed in a 10 mm tube, was 80% phosphoric acid (2 μL) in CD_3OD (2 mL), and chemical shift values are reported relative to this reference.

Materials. HEDP and $UO_2(OAc)_2-2H_2O$ were purchased from Aldrich (Aldrich Co, St. Louis, MO). Concentrated 4.2×10^{-4} M stock solutions of HEDP and UO_2^{2+} were obtained by dissolving the required amount of HEDP and $UO_2(OAc)_2-2H_2O$.

The pH was adjusted by using perchloric acid or sodium hydroxide and was controlled throughout the experiments. The pH of the solution in the cell is measured with a conventional pH meter (LPH430T). For each solution, UO_2^{2+} and HEDP concentration, pH, and ionic strength were fixed (by using a 0.1 M sodium perchlorate solution) and controlled. The values for stepwise protonation constants of HEDP (H_4L) corresponding to this ionic strength are[24] $pK_a = 1.8$ (H_3L^-), 2.7 (H_2L^{2-}), 7 (HL^{3-}), and 11.2 (L^{4-}). All fluorescence measurements were performed at 20 °C.

Solutions for the ESI-MS measurements were prepared from 2 mL of UO_2^{2+} aqueous solution (4.2×10^{-5} M) mixed with a precise volume of HEDP solution required to give metal-to-ligand ratios UO_2^{2+}/HEDP in the range 0−5.

In ATR-IR experiments, the solid sample was prepared by evaporing to dryness the solution containing the UO_2^{2+}−HEDP complex at 95 mM in CD_3OD.

All chemical used were reagent grade, and Millipore water was used throughout the procedure.

Results and Discussion

Uranyl speciation in aqueous solution is very complex[25−27] because of the presence of numerous species depending on the concentration and pH, which has been widely studied. Different species can be observed, ranging from free uranyl (UO_2^{2+}) at acidic pH to the carbonato complex $(UO_2(CO_3)_3)^{4-}$ at basic pH going through hydroxo and polymeric complexes. So, in the present paper, all experiments were carried out at pH ≤ 5.5, the higher value being the one of the renal compartment and because above this pH the system becomes very complex (see speciation diagram of uranium(VI) in Supporting Information). For example, the $(UO_2)_3(OH)_5$ masks the complex fluorescence at pH 7, and the presence of carbonato complex (not fluorescent) limits also the exploitation of such data. Therefore, to simplify the speciation diagram, it is necessary to work at lower concentration, that is, $[U(VI)] = 4.2 \times 10^{-8}$ M, which is very close to the limit of detection of TRLIF and much too low for ES-MS studies. So, one study has been done at pH 7.

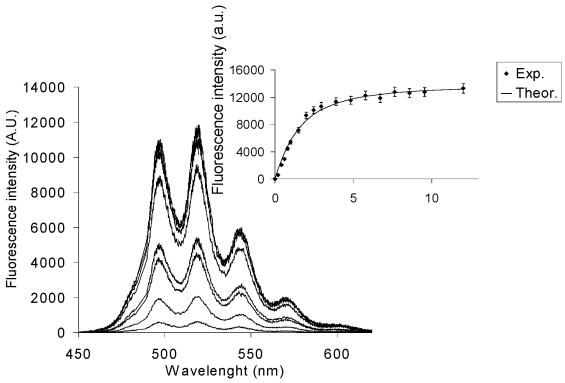

Figure 1. Spectrofluorimetric titration of a solution of HEDP (4.2×10^{-7} M) by an aqueous solution of UO_2^{2+} in 0.1 M $NaClO_4$, pH = 5: from bottom to top, 0, 0.2, 0.4, 0.8, 1, 2, 4, 8, and 12 equiv of UO_2^{2+}. The inset shows the experimental (◆) and theoretical (—) uranyl fluorescence intensity as a function of $[UO_2^{2+}]$/[HEDP] molar ratio at $\lambda_{exc} = 266$ nm and $\lambda_{em} = 519$ nm.

Numerous studies have been carried out on uranium speciation by TRLIF.[28−30] Hence, TRLIF experiments are based on the spectrotemporal analysis of the fluorescence signal. Sensitivity down to 10^{-9} M in speciation studies (the composition of the medium being fixed by real conditions) can be achieved. The advantages of this method are related to the triple resolution of TRLIF: (i) excitation resolution by the proper choice of the laser wavelength (N_2, tripled or quadrupled Nd :YAG, dye, OPO, ...); (ii) emission fluorescence, which gives characteristic spectra of the fluorescent cation (free or complexed); (iii) fluorescence lifetime, which is characteristic of its environment (complexation, quenching).

Fluorescence Studies of the Complex. The method is based on the study of the fluorescence of the UO_2^{2+}−HEDP complex by progressive additions of UO_2^{2+} in a HEDP solution, which leads to an increase of fluorescence until saturation. The reverse way can also be used.[31] A typical experiment is shown in Figure 1, where the fluorescence of complex (4.2×10^{-7} M HEDP in H_2O) at pH 5 has been plotted as a function of UO_2^{2+} concentration at a fixed ionic strength ($I = 0.1$).

The fluorescence spectrum of the aqueous uranyl ion reflects the symmetrical vibration of the U−O bond. The observed emission bands correspond to the electronic transition $S_{11} \rightarrow S_{00}$ (473 nm) and $S_{10} \rightarrow S_{0\nu}$ for $\nu = 0-4$ (488, 510, 535, 560 and 587 nm).[32−33] With increasing HEDP concentration, a bathochromic shift of the uranyl emission

(24) Smith, R. M.; Martell, A. E. *NIST Critically Selected Stability Constants of Metal Complexes Database*, version 4.0; U. S. Department of Commerce, National Institute of Standards and Technology: Gaithersburg, MD, 1997.
(25) Katz, J. J.; Seaborg, G. T.; Morss, L. R. *The Chemistry of the Actinide Elements*; Chapman and Hall: London/New York, 1986; Vol. 2.
(26) Based on the complexing constant of the Organization for Economic Cooperation and Development−Nuclear Energy Agency (O.E.C.D−N.E.A) thermodynamical database.
(27) Grenthe, I.; Fuger, J.; Konings, J. M.; Lemire, R. J.; Muller, A. B.; Nguyen Trung, J.; Wanner, H. *Chemical Thermodynamics of Uranium*; N.E.A-TDB, O.E.C.D., Nuclear Energy Agency Data Bank; North-Holland: Amsterdam, 1992.
(28) Couston, L.; Pouyat, D.; Moulin, C.; Decambox, P. *Appl. Spectrosc.* **1995**, *49*, 3, 349.
(29) Dewberry, R. A. *Nucl. Instrum. Methods A* **1998**, *403*, 383.
(30) Beitz, J. V.; Williams, C. W. *J. Alloys Compd.* **1997**, *250*, 375.
(31) Moulin, C.; Reiller, P.; Beaucaire, C.; Lemordant D. *J. Colloid Interface Sci.* **1993**, *157*, 411.

Table 1. Conditional Constant of Complex UO_2^{2+}−HEDP for $I = 0.1$ and 1:1 Complex Stoichiometry

pH	conditional constant ($\log \beta^0 \pm \sigma$)
1	4.7 ± 0.3
2	4.7 ± 0.5
4	7.5 ± 0.8
5	6.7 ± 0.4
7	7.7 ± 0.3

takes place, which is attributed to a UO_2^{2+}−HEDP complexation. The strongest shift is observed at high UO_2^{2+} concentrations and reaches a maximum of 9 nm (Figure 1). Additionally, a strong enhancement of the fluorescence intensity and an increased fluorescence lifetime occurs when the HEDP is present as will be seen later.

Titration and Stability Constant. When experimental results are used, it is possible to reach the complex stoichiometry and the conditional constant by a nonlinear regression fit at $\lambda_{max} = 519$ nm (excitation at 266 nm). The model is based on the complexation reaction in solution:

$$M + nL \leftrightarrow ML_n \quad (1)$$

The conditional constant, β^0_n, can be expressed in a particular ionic medium by

$$\beta^0_n = [ML_n]/[M][L]^n \quad (2)$$

where M represents free UO_2^{2+} and L is the organic ligand.

Considering a complex of 1:1 stoichiometry, the fluorescence intensity can be described by the following equation:

$$I_{tot} = I_M(1 - \beta^0[L]) + \beta^0[L]I_{ML} \quad (3)$$

By using eq 3, we can fit the titration curve (inset in the Figure 1) and calculate the conditional constant of the complex. The inset in Figure 1 shows, at pH 5, the experimental and theoretical fluorescence curves obtained for the UO_2^{2+}−HEDP system. If another model is applied to this system (for example, a 1:2 complex or more), the data observed do not fit. Results obtained for the complexation constant ($\log \beta^0$) as a function of pH are summarized in Table 1. Calculated conditional constants were averaged from 10 experiments. A good agreement is observed between normal and inverse titration curves, supporting their reliability. The standard deviation was determined from all conditional constants calculated for each titration. The species distribution plots obtained from these data are shown in Figure 2. From the species distribution curves, the predominant complex present under these experimental conditions is MH_2L, and a mixture of MH_3L and MH_2L exists between pH 1.2 and 3.7, which is compatible with experiments.

The stability constants can be calculated for the species MH_3L and MH_2L by the expressions

$$K_1 = K_{a1}{}^*\beta^0{}_1 \quad \text{and} \quad K_2 = K_{a1}{}^*K_{a2}{}^*\beta^0{}_2$$

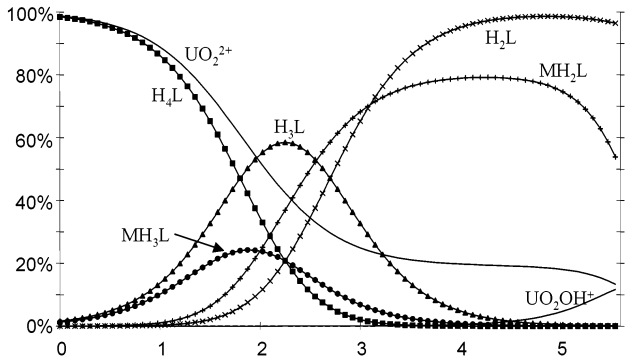

Figure 2. Species distribution plot for an aqueous solution containing UO_2^{2+} and HEDP at a ratio of 1:1 metal/ligand (M/L) with $[UO_2^{2+}] = 4.2$ μM and $I = 0.1$.

where K_{a1} and K_{a2} represent the protonation constant of HEDP ($10^{1.8}$ and $10^{2.7}$) and β^0 is the conditional constant. The values found are $K_1 = 10^{6.5}$ for MH_3L and $K_2 = 10^{11.5}$ for MH_2L. The latter one can be compared with the value obtained by Nash, $10^{11.8}$, using extraction techniques.[22] Compared with diphosphonates, such as methanediphosphonic acid (MDPA) or aminomethylenediphosphonates (MAMDP, AMDP),[22] the conditional constant obtained with the MH_2L species at pH 4−5 between UO_2^{2+} and HEDP is similar but the stability constant is less compared to MAMDP and AMDP ($10^{17.4}$ and $10^{18.5}$), probably because of the presence amino groups that stabilize the complex as suggested by the author. Although this system is very difficult to analyze at pH 7, a titration experiment has been performed with $[U(VI)] = 4.2 \times 10^{-8}$ M (close to limit detection of TRLIF for speciation studies). The conditional constant found is $\log \beta^0_3 = 7.7 \pm 0.3$, and the stability constant is $K_3 = 10^{19.1}(K_{a1}{}^*K_{a2}{}^*K_{a3}{}^*\beta^0_3)$ between HEDP and U(VI). But it is impossible to know the type of formed complex, that is, what species of uranyl react with HEDP, because fluorescence signals obtained are very weak.

Lifetime of the Complex. Moreover, the fluorescence evolution as a function of time shows two decay components with fluorescence lifetime different from UO_2^{2+}, confirming the formation of UO_2^{2+}−HEDP complexes. According to the speciation diagram (Figure 1) and in the absence of the ligand, two species are present at pH = 5, UO_2^{2+} ($\tau = 2$ μs) and UO_2OH^+($\tau = 80$ μs).[34] In the presence of the ligand and by a nonlinear regression fit, two lifetimes of 110 μs and 80 μs were found compatible, respectively, with the complex UO_2^{2+}−HEDP and UO_2OH^+ at pH = 5. The presence of UO_2OH^+ shows that it is mainly UO_2^{2+} that is complexed with HEDP. Indeed, it is not possible to have another complex because fluorescence wavelengths correspond to the species UO_2OH^+.

The lifetime measurements and the wavelength at different pH are summarized in Table 2. It is well established that uranyl ion is a hard Lewis acid and has a high affinity for hard donor groups such as the negative or neutral oxygen donors.[35] There is a competition between the protonation and

(32) Bell, J. T.; Biggers, R. E. *J. Mol. Spectrosc.* **1968**, *25*, 312.
(33) Rabinowitsch, E.; Belford, R. L. *Spectroscopy and Photophysics of Uranyl Compounds*; Pergamon Press: Oxford, U.K., 1964.
(34) Moulin, C.; Decambox, P.; Moulin, V.; Decaillon, J. G. *Anal. Chem.* **1995**, *67*, 348.
(35) Pearson, R. G. *J. Am. Chem. Soc.* **1963**, *85*, 3533.

Table 2. Spectroscopic Data of the Uranyl−HEDP Complex at Various pH

pH	fluorescence wavelengths (nm)	τ (μs) $\pm$ σ	HEDP major species	pK_a[23]
1	494, 516, 540, 566	20 ± 5	H_4L	
2	496, 519, 545, 572	22 ± 5	H_3L^-	1.8
		60 ± 10		
4	496, 519, 545, 572	110 ± 5	$H_2L_2^-$	2.7
5	496, 519, 545, 572	110 ± 5	$H_2L_2^-$	2.7
7	500, 520, 546, 573		HL^-	7

metalation. Therefore, at pH = 1, it is not surprising to have a complexation between uranyl ion and HEDP even if the ligand is not much activated. This aspect is more visible at pH = 2 where the complex lifetime increases (22 to 60 μs) in inverse or normal titration. At pH 7, it is impossible to measure the lifetime of the complex because of the very weak fluorescence signal.

It is interesting to note that the fluorescence lifetime of HEDP−uranyl complex is similar to that of phosphoric acid−uranyl complex (used as complexing reagent for analytical determinations) at pH 5. Therefore, HEDP is also a potential candidate to analytical application in the nuclear fuel cycle, as well as for biological applications. Moreover, the same increase of fluorescence is observed (2 orders of magnitude) by adding stoichiometric amount of HEDP compared to classical analytical media ratio for uranium determination (H_3PO_4 5%).

Electrospray Mass Spectrometry (ES-MS). First developed for biological applications because it allows for very high mass by making multicharged species, electrospray mass spectrometry (ES-MS) is a powerful tool for speciation studies in solution because of its soft mode of ionization. Hence, it is possible to generate ions at atmospheric pressure to mass detection working at reduced pressure. However, mechanisms taking place in the source are very complex, and special care should be taken in terms of the interpretation of results. For purposes of convenience, the process can be divided into three steps: droplet formation, droplet shrinkage, and gaseous ion formation. It can be used basically in two different ways, each giving access to a different kind of information: (i) Full scan simple MS spectra can be recorded with soft conditions to detect the complexes that are present in the infused solution.[36] (ii) Once the complexes of interest are isolated in the gas phase, the structural information (without any influence of the solvent) can be obtained.[37] In this part, ES-MS is used to confirm the stoichiometry and to determine stability constant of the UO_2^{2+}−HEDP complex.

In the positive mode, at low voltage cone, the spectra reveal three major peaks at *m*/*z* 575−577, 593−595, and 681, which can be respectively attributed to $[(UO_2)(H_3L)(HClO_4)]^+$, $[(UO_2)(H_3L)(HClO_4)(H_2O)]^+$, and $[(UO_2)(H_3L)(H_4L)]^+$ at pH 1 or 2. The classic cluster of complexes is formed in solution with H_2O and $HClO_4$. By using a higher cone voltage, new peaks are observed at *m*/*z* = 475, 493, and 511, which are compatible with the formation of

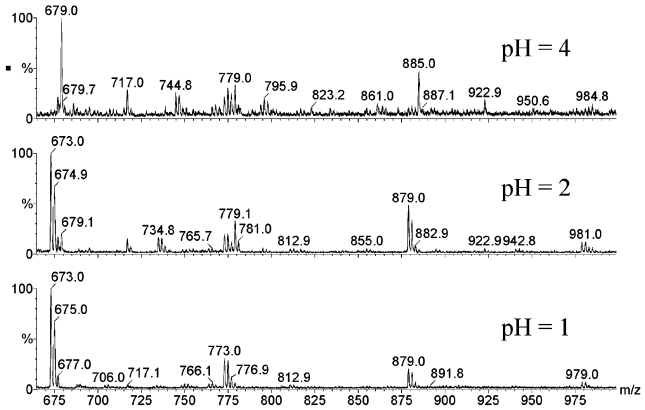

Figure 3. Negative ES-MS spectra of a solution of UO_2^{2+} (4.2×10^{-5} M in 0.1 M $NaClO_4$) at pH = 1, 2, and 4 in the presence of 5 equiv of HEDP with cone voltage of 30 V.

Table 3. Assignments of the Peaks Observed in ES-MS Positive and Negative Mode at pH = 1 or 2 (HEDP = H_4L)

m/*z*	assignment
207	$[(H_4L) + H]^+$
297	$[(H_4L)(H_2O)_5 + H]^+$
413	$[(H_4L)_2 + H]^+$
430	$[(H_4L)_2(H_2O) + H]^+$
475	$[(UO_2)(H_3L)]^+$
493	$[(UO_2)(H_3L)(H_2O)]^+$
511	$[(UO_2)(H_3L)(H_2O)_2]^+$
575−577	$[(UO_2)(H_3L)(HClO_4)]^+$
593−595	$[(UO_2)(H_3L)(HClO_4)(H_2O)]^+$
681	$[(UO_2)(H_3L)(H_4L)]^+$
699	$[(UO_2)(H_3L)(H_4L)(H_2O)]^+$
781−783	$[(UO_2)(H_3L)(H_4L)(HClO_4)]^+$
887	$[(UO_2)(H_3L)(H_4L)_2]^+$
305−307	$[(H_3L)(HClO_4)]^-$
405−407	$[(H_3L)(HClO_4)_2]^-$
511−513	$[(H_3L)(H_4L)(HClO_4)]^-$
567−573	$[(UO_2)(ClO_4)_3]^-$
673−677	$[(UO_2)(H_3L)(ClO_4)_2]^-$
773−779	$[(UO_2)(H_3L)(ClO_4)_2HClO_4]^-$
779−781	$[(UO_2)(H_2L)(H_4L)(ClO_4)]^-$
879−883	$[(UO_2)(H_3L)(H_4L)(ClO_4)_2]^-$
979−985	$[(UO_2)(H_3L)(H_4L)(ClO_4)_2(HClO_4)]^-$

complexes of formula $[(UO_2)(H_3L)]^+(H_2O)_n$, n = 0, 1, and 2. At pH = 4, the complex formed is neutral because of the state of protonation of HEDP (H_2L^{2-}). So, it is not surprising that it is not observed in the spectra.

In the negative mode, ES-MS of the UO_2^{2+}−HEDP system shows three major peaks at 673−677, 773−779, and 879−883 *m*/*z* corresponding, respectively, to $[(UO_2)(H_3L)(ClO_4)_2]^-$, $[(UO_2)(H_3L)(ClO_4)_2HClO_4]^-$, and $[(UO_2)(H_3L)(H_4L)(ClO_4)_2]^-$ at pH = 1 or 2 (Figure 3). Other peaks are observed but correspond to the ligand alone (H_3L^-) or with $HClO_4$ or H_4L as a cluster. At pH = 4, two peaks are observed at *m*/*z* = 679 and 779−781 corresponding, respectively, to $[(UO_2)(H_2L)(H_3L)]^-$ and $[(UO_2)(H_2L)(H_4L)(ClO_4)]^-$. So, the neutral complex can be observed by the formed cluster with ClO_4^- or H_3L^-. Moreover, the peak at 779−781 *m*/*z* corresponding to $[(UO_2)(H_2L)(H_4L)(ClO_4)]^-$ is also present at pH = 2 in the negative spectra, which confirms the obtained results in fluorescence (lifetime) where the value is an average of MH_3L and MH_2L species. Table 3 summarizes the assignments of the peaks in positive and negative mode, which also allow us to confirm the complex stoichiometry (1:1)

(36) Gabelica, V.; Galic, N.; Pauw, E. D. *J. Am. Soc. Mass Spectrom.* **2002**, *13*, 946.
(37) Colette, S.; Amekraz, B.; Madic, C.; Berthon, L.; Cote, G.; Moulin C. *Inorg. Chem.* **2002**, *41*, 7031.

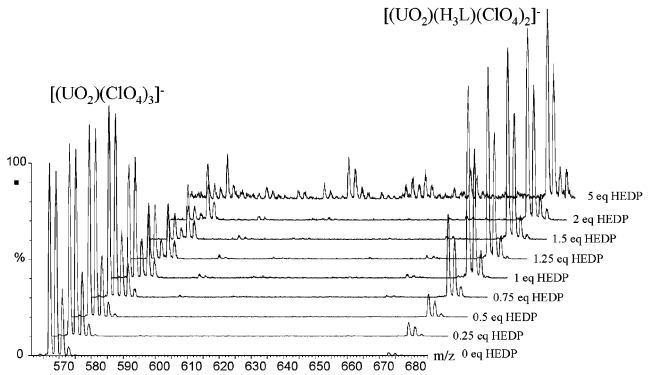

Figure 4. ES-MS spectra of uranyl as a function of [HEDP]/[UO_2^{2+}] molar ratio at 4.2×10^{-5} M, pH = 2 in perchloric acid. Cone voltage was 30 V. Additions of HEDP at 4.2×10^{-3} M were made to give molar ratios of 0, 0.25, 0.5, 0.75, 1, 1.25, 1.5, 2, and 5.

that was found in TRLIF. Indeed, the spectra, in positive or negative mode, reveal the formation in solution of a classic cluster of complexes with $HClO_4$ and ClO_4^- or H_4L and therefore do not suggest a complex stoichiometry of 1:2. These clusters are not implicated in a direct complexation but rather in the second coordination sphere by hydrogen bonding. To confirm the assignments, a MS/MS fragmentation was performed, for example, at $m/z = 681$ corresponding to the complex $[(UO_2)(H_3L)(H_4L)]^+$. The result obtained shows the disappearance of the H_4L cluster to the benefit of the complex $[(UO_2)(H_3L)]^+$ at m/z 475.

Titration in ES-MS. Negative mode electrospray ionization experiments have been also used to evaluate the conditional constant by titration at pH = 2 (Figure 4). Indeed, several studies have shown a good agreement between solution-phase and gas-phase ionic abundance for metal complexes present in thermodynamic equilibrium in solution.[38−40]

Without HEDP, the spectra show a peak at m/z 567−573 attributed to $[(UO_2)(ClO_4)_3]^-$, and progressive additions of HEDP induce the formation of the 1:1 complex at m/z 673−679, which is compatible with $[(UO_2)(H_3L)(ClO_4)_2]^-$ (Figure 4). In each case, the chloride isotopic ratio (^{35}Cl 66%, ^{37}Cl 33%) is clearly observed and explains the observed mass range. From these data, a conditional constant can be calculated.[36,41] The method is based on the relation between the peak intensity (I_M) and the concentration:

$$[M] = t_M * I_M \qquad (4)$$

where t_M is the transfer coefficient.

Assuming that this coefficient is the same for all the uranium species, it is possible to reach the concentration ratio from the peak intensity ratio:

$$[(UO_2)(H_3L)(ClO_4)_2]^-/[(UO_2)(ClO_4)_3]^- = \sum I([(UO_2)(H_3L)(ClO_4)_2]^-)/\sum I([(UO_2)(ClO_4)_3]^-) \qquad (5)$$

(38) Andrew, R. S. R.; Ikonomou, M. G.; Thompson, J. A. J.; Orians, K. *J. Anal. Chem.* **1998**, *70*, 11, 2225.
(39) Wang, H.; Agnes, G. R. *Anal. Chem.* **1999**, *71*, 17, 3785.
(40) Wang, H.; Agnes, G. R. *Anal. Chem.* **1999**, *71*, 19, 4166.
(41) Whittal, R. M.; Ball, H. L.; Cohen, F. E.; Burlingame, A. L.; Prusiner, S. B.; Baldwin, M. A. *Protein Sci.* **2000**, *9*, 332.

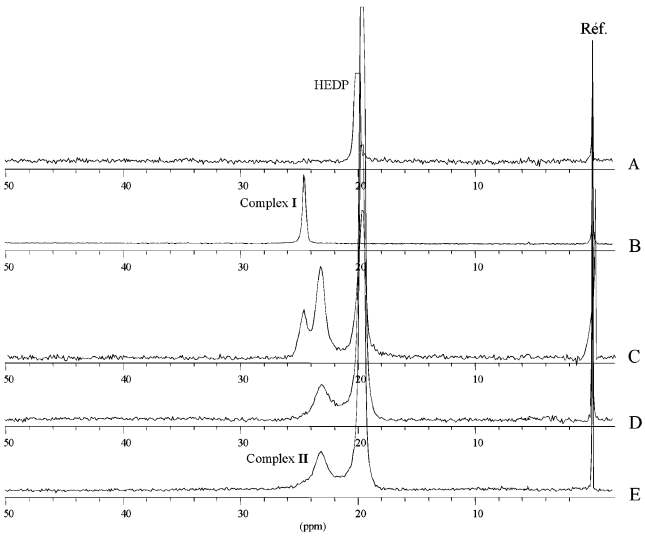

Figure 5. ^{31}P NMR spectra of HEDP 20 mM (A) and UO_2^{2+} titrated with HEDP at $R = 1$ (B), 2 (C), 5 (D), and 10 (E) at $T = 293$ K in CD_3OD.

Therefore, the free HEDP, UO_2^{2+}, and the complex concentrations can be calculated allowing us to reach to the conditional constant. By using the Debye−Hückel law, we can recalculate the conditional constant at $I = 0.1$, which corresponds to the ionic strength in the TRLIF experiment. The average value found of $\log \beta^0 = 4.2 \pm 0.5$ is in good agreement with the one obtained by TRLIF (4.7 ± 0.5). This result confirms that solution-phase characteristics can be directly reflected in ESI mass spectra. No titration can be done at pH 4 or 5 because of the simultaneous distribution of the complex on the peaks m/z 679 and 779−781.

So, in weakly acidic medium, at a low HEDP concentration in the solution (10^{-5}−10^{-7} M), the complex $[UO_2(H_3L)]$ is formed, although in weakly alkaline medium, the complex has the composition $[UO_2(H_2L)]$.

NMR Investigation. NMR was used to investigate different aspects of the coordination dynamics of the metal−ligand system. The ^{31}P NMR spectroscopy appears to be the best tool to answer the following question: what is the influence of HEDP concentration on the formed complex.

Because addition of HEDP to concentrated aqueous solutions of UO_2^{2+} in D_2O resulted in a precipitation of complex, NMR experiments were carried out in CD_3OD. Up to a ligand-to-metal ratio (R) of 1, one complex was formed (complex **I**), while increasing the R value above 2 resulted in the formation of another complex (complex **II**), which appears at lower fields (Figure 5). At room temperature, NMR spectra showed that the complexation of HEDP to UO_2^{2+} is achieved through the coordination of the P−O^- chelating site of HEDP because of the downfield shift of ^{31}P ($\Delta\delta = 5$ and 3.5 ppm). Indeed, these spectra in which uranyl is complexed by the phosphonate ligands were characterized by three distinct ^{31}P resonances corresponding to the free and complexed ligand species. The approximate chemical shifts for the free and bound ligands are 19.9 (HEDP), 23.4 (complex **II**), and 24.8 ppm (complex **I**). The Figure 5B reveals only the complex **I** and by successive addition of HEDP, the complex **I** disappears to profit the

Scheme 1. Proposed Structure of the Uranyl−HEDP Complex

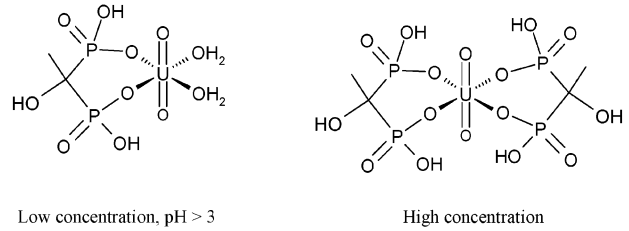

Low concentration, pH > 3 High concentration

complex **II** (Figure 5C−E). Compared to the reference (H_3PO_4), the integrated areas of these two complexes in the NMR spectra show that the dominant metal−ligand stoichiometry is 1:1 for $R = 1$ and 1:2 for $R \geq 2$. The concentration of free HEDP and complexed species can be calculated. For example, in the case of the Figure 5C where it is a mixture of 1:1 and 1:2 complex, the values found are 40% of free HEDP (16 mM), 25% of complex **II** (5 mM)**,** and 35% of complex **I** (14 mM). Therefore, when the ratio *R* increases the 1:1 complex decreases to profit the 1:2 complex and inversely.

So, at high HEDP concentrations (10^{-2} M) and in CD_3OD, only $[UO_2(H_2L)]$ (1:1) or a mixture, $[UO_2(H_2L)_2]$ (1:2) and $[UO_2(H_2L)]$, of complexes are formed, but if the HEDP concentration is superior to 10^{-2} M, only the 1:2 complex is observed. Even if these experiments were performed in CD_3OD, it is not likely excluded that this behavior occurs in the aqueous solution. To confirm the proposed structure (Scheme 1), low-temperature ^{31}P NMR experiments have been performed (Figure S3 in Supporting Information). The results show only one ^{31}P signal and confirm the 1:1 complex proposed (six-membered ring) due to the plane of symmetry through the central carbon.

ATR-IR Spectroscopy. The dynamic nature of metal−ligand interactions in solution requires that the proposed structure is at best an average representation of the complex present in the solution. The ATR-IR (attenuated total reflection in infrared) spectra of metal complexes in the solid state give specific structural information concerning a possible configuration of the complex. Hence, selected details of the structure of coordination compounds in the solid state can provide useful guidance for the interpretation of most probable structures of complexes in solution.

The ATR-IR was recorded between 4000 and 650 cm^{-1}. ATR-IR spectra of the UO_2^{2+}−HEDP complex differ in certain regions compared to HEDP alone and can be assigned on the basis of previous results from the literature.[42] Figure 6 shows zoom spectra between 1370 and 650 cm^{-1} where the vibration bands are mainly changed.

The broad band in the 3500−2410 cm^{-1} region of the HEDP spectra, which represents the OH stretching region (the α-hydroxy group and protonated phosphonates), disappears to the profit of a broad band centered at 2450 cm^{-1}. Vibration bands assigned to PO_3 symmetric and asymmetric stretching modes are observed in the 1080−1250 cm^{-1} region for HEDP and in the case of the complex are shifted to the

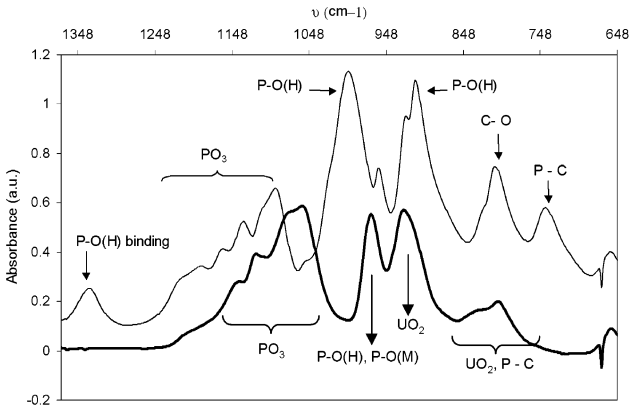

Figure 6. ATR-IR spectrum for HEDP alone (−) and UO_2/HEDP complex (−) at room temperature.

1000−1200 cm^{-1} region. Vibration bands assigned to the P−C asymmetric stretching modes are observed at 737 cm^{-1} for HEDP, while they are shifted in the broad band around 800 cm^{-1} for the complex. The band at 1330 cm^{-1} assigned to the P−O(H) binding mode disappears. Vibration bands assigned to the (P−O)H symmetric and asymmetric stretching modes are observed in the 1000−900 cm^{-1} region for HEDP, while the (P−O)M and (P−O)H vibrations are observed at about 966 cm^{-1}. The frequencies due to UO_2 vibrations are seen at 922 (asymmetric) and 831 cm^{-1} (symmetric).[43−45]

So, the nature of metal−ligand coordination depends on the characteristics of the metal ion and on the pH. The ATR-IR spectra have shown that the ligand coordinates UO_2^{2+} through the $P-O^-$ chelating site. The mass spectra can give structural information on the coordination between the complex and H_2O. For the 1:1 complex, two water molecules are localized in the outer sphere. In the case of another phosphonate derivative (methylphosphonate), Clearfield and co-workers[46] have resolved the crystal structure of the $UO_2(O_3PCH_3)$ complex and confirmed the coordination through the connectivity of the metal−PO_3 groups. Therefore, two structures can be proposed according to the concentration and the pH (Scheme 1).

Of course, to confirm these hypotheses, the crystallographic structure of the complex must be resolved, and this point is currently in progress.

Selectivity of the Complex. The potential role of HEDP is to reduce effectively the fixation of uranium in its target organs: bone and kidney. So, it is very important to study the stability of the complex toward the other metal cations and, in particular, those present in biological fluids in humans that are present at much higher concentration than uranyl and could compete for HEDP complexation. The selectivity of the complex can be evaluated by competitive binding with those ions. The method is based on TRLIF experiments and consists in adding a competing metal cation (M^{n+}) in the presence of the UO_2^{2+}−HEDP complex. A decrease of the complex fluorescence will be observed if those metals form

(42) Thomas, L. C. *The Identification of Functional Groups in Organophosphorus Compounds*; Academic Press: London, 1994.

(43) Conn, G. K. T.; Wu, C. K. *Trans. Faraday Soc.* **1938**, *34*, 106.
(44) Jones, L. H.; Penneman, R. A. *J. Chem. Phys.* **1953**, *21*, 542.
(45) Jones, L. H. J. *Chem. Phys.* **1955**, *2*, 2105.
(46) Grohol, D.; Gingl, F.; Clearfield, A. *Inorg. Chem.* **1999**, *38*, 751.

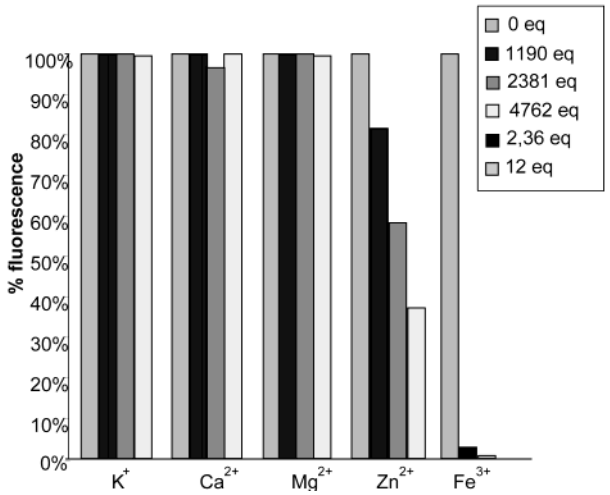

Figure 7. Selectivity of $[UO_2(H_2L)]$ complex in the presence of the metal cations with different ratios: 0, 1190, 2381, and 4762 equiv of K^+, Ca^{2+}, Mg^{2+}, and Zn^{2+} and 0, 2.36, and 12 equiv of Fe^{3+}. $[UO_2(H_2L)] = 4.2 \times 10^{-7}$ M; $[NaClO_4] = 0.1$ M; pH = 5.

a new complex with HEDP. So, a representative concentration of competing metal cations, such as K^+ (10^{-3}−10^{-2} M), Ca^{2+} (10^{-3}−10^{-2} M), Mg^{2+} (10^{-3}−10^{-2} M), Zn^{2+} (10^{-3}−10^{-2} M), and Fe^{3+} (10^{-6}−10^{-5} M), has been added to the solution of the 1:1 complex (4.2×10^{-7} M) at pH = 5. Figure 7 shows the results obtained. The UO_2^{2+}−HEDP complex lifetime has been examined to verify that no lifetime variation exists because of the addition of complexing cations (which would indicate dynamic quenching and not complexation (static quenching)).

The data reveal that K^+, Ca^{2+}, and Mg^{2+} did not influence the stability of the UO_2^{2+}−HEDP complex, but Zn^{2+} affected slightly the complex, and Fe^{3+} dramatically decomplexed HEDP from uranyl. These data are in good agreement with the literature[21,47−49] because the formation constant between HEDP and metal ions is smaller than the thermodynamic constant of the $[UO_2H_2L]$ species ($10^{11.5}$) except with Fe^{3+}. Indeed, the formation constants with HEDP are about 100.7 for Na^+, 100.6 for K^+, 10^6 for Mg^{2+} and Ca^{2+}, 10^{8-11} for Zn^{2+}, and $>10^{16}$ for Fe^{3+} in the same ionic strength and temperature.

So, the UO_2^{2+}−HEDP complex presents a good stability even in the presence of excess of other metals, except Zn^{2+} and Fe^{3+}. However, these two metal are not free in the organism at high concentrations. Indeed, iron is mainly complexed with the protein transferin and ferritin, whereas zinc is trapped by metallothioneine. So, HEDP appears to be a good candidate for the decorporation of uranyl ions. Further studies are under investigation to measure the selectivity of HEDP in the human plasma by mass spectrometry to examine the complex behavior.

Conclusion

Spectroscopic analysis, especially mass spectrometry and fluorescence, can provide many detailed characteristics of the complexes formed, while ATR-IR and NMR spectroscopy has also proved to be powerful tools for the structural investigations. Results allowed us to elucidate the stability constant, the stoichiometry, and the structural details of UO_2^{2+} complexation with HEDP and, especially, the ratio between uranyl and HEDP, which is an important factor for biological use. The complex UO_2^{2+}−HEDP has a good stability toward many metals, except for Fe^{3+}. Therefore the application of this molecule in decorporation seems very interesting in particular for bone uranium removal. The design of a new organophosphate with binding activity toward UO_2^{2+} is currently under study. Nevertheless, the present data suggest that HEDP is a promising model for the binding of toxic metals, and the fluorescence properties of the complex suggest possible applications in other domains, environmental analysis, for example.

Acknowledgment. This work was supported by the "Nuclear Toxicology" program of the Commissariat à l'Energie Atomique (CEA) for which grateful acknowledgment is made, and acknowledgment is also made for financial support and for a postdoctoral fellowship to C. Jacopin.

Supporting Information Available: Figure S1 giving the speciation diagram of UO_2^{2+} at 4.2×10^{-5} and 4.2×10^{-7} M from the O.E.C.D. databank; Figure S2 giving ES-MS spectra of 4.2×10^{-5} M UO_2^{2+} in 0.1 M $NaClO_4$ with 5 equiv of HEDP at pH = 1, 2, and 4; Figure S3 giving NMR experiments at low temperature in CD_3OD. This material is available free of charge via the Internet at http://pubs.acs.org.

IC0343509

(47) Hiroko, W.; Quintus, F. *Anal. Chem.* **1972**, *44*, 9, 1640.
(48) Kabachnik, M. I.; Lastovskii, R. P.; Medved, T. Ya.; Medynstev, V. V.; Kolpakova, I. D.; Dyatlova, N. M. *Proc. Acad. Sci. USSR* **1967**, *177*, 1060.
(49) Smith, R. M.; Martell, A. E. *Critical Stability Constants*; Plenum Press: New York, 1982; Vol. 6.